CMS ECAL Monitoring and Calibration in LHC Run 2

Tanmay Mudholkar

On behalf of the CMS Collaboration

CALOR 2018, Session 1, May 21
Eugene, Oregon

Outline

1. Introduction
   - ECAL Building Blocks
2. Calibration
   - Inter-calibration: Motivation
   - Inter-calibration: Methods
   - Inter-calibration: Results
   - Preshower Calibration
3. Monitoring and Validation using physics events
   - Motivation and methods
   - Energy scale
   - Shower shape
4. Summary

Outline

1. Introduction
   - ECAL Building Blocks
2. Calibration
   - Inter-calibration: Motivation
   - Inter-calibration: Methods
   - Inter-calibration: Results
   - Preshower Calibration
3. Monitoring and Validation using physics events
   - Motivation and methods
   - Energy scale
   - Shower shape
4. Summary

Schematic Diagram

The CMS Electromagnetic Calorimeter consists of 75848 scintillating $PbWO_4$ crystals and 137216 sampling Si strips with Pb absorber.

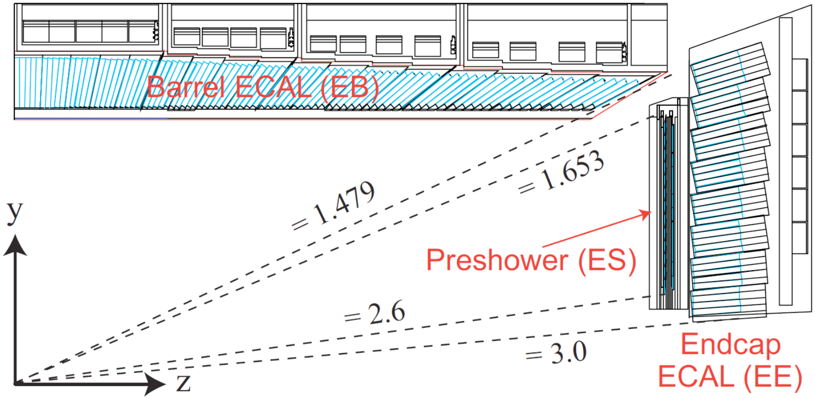

Building Blocks: ECAL Barrel + Endcaps

The CMS Electromagnetic Calorimeter consists of 75848 scintillating $PbWO_4$ crystals and 137216 sampling Si strips with Pb absorber.

Barrel APDs

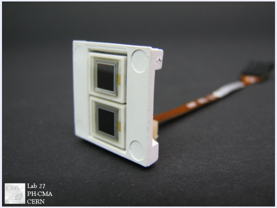

- Attached to 61200 crystals
- Crystal dimensions: $2.2 \times 2.2 \times 23\ \mathrm{cm}^3$
- Designed to operate at 4 T, gain 50

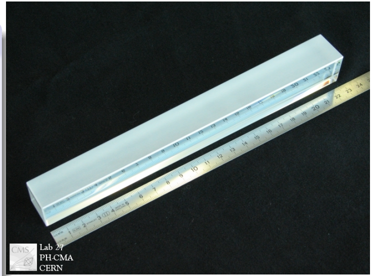

$PbWO_4$ crystals: $\rho = 8.28\,\mathrm{g\,cm^{-3}}$

$X_0 = 0.89\,\mathrm{cm}$, $R_M = 2.19\,\mathrm{cm}$

Endcap VPTs

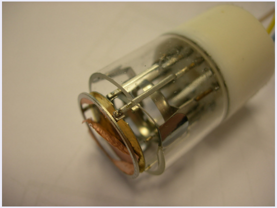

- Attached to 14648 crystals
- Crystal dimensions: $2.9 \times 2.9 \times 22\ \mathrm{cm}^3$ (front face)
- Higher radiation tolerance, gain 10

Building Blocks: ECAL Preshower

The CMS Electromagnetic Calorimeter consists of 75848 scintillating $PbWO_4$ crystals and 137216 sampling Si strips with Pb absorber.

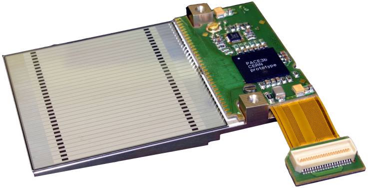

Assembled Preshower Module used in beam tests

ECAL Preshower

- ECAL Preshower consists of four planes, two in front of each endcap
- Thickness of lead plates: $\approx 3X_0$
- Each Si sensor consists of 32 "strips", oriented along X in one plane and along Y in the other at both endcaps
- Strip size: $2.0 \times 63 \times 0.3\ \text{mm}^3$

Higher spatial resolution helps distinguish genuine high-energy photons from close photon pairs (*e.g.* those resulting from π^0-decay).

Monitoring and Calibration

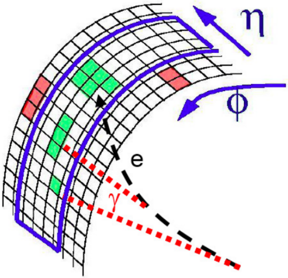

An algorithm identifies a list of crystals (a “supercluster”) in which a photon or electron from the collision is likely to deposit energy.

$$E_{e,\gamma} = F_{e,\gamma} \times \left[G\left(\eta\right) \times \left\{ \sum_{i\ \in\ \mathrm{SC}} S_i\left(t\right) \times \boxed{C_i} \times A_i \right\} + \boxed{E_{\mathrm{preshower}}} \right]$$

This talk focuses on how we obtain the inter-calibration coefficients C_i, and validate and monitor physics quantities over the data-taking period.

Outline

1. Introduction
   - ECAL Building Blocks

2. Calibration
   - Inter-calibration: Motivation
   - Inter-calibration: Methods
   - Inter-calibration: Results
   - Preshower Calibration

3. Monitoring and Validation using physics events
   - Motivation and methods
   - Energy scale
   - Shower shape

4. Summary

Inter-calibration: motivation

- The laser monitoring signal L is used to correct the scintillation signal S for short term effects (*e.g.* radiation-induced damage to crystals during fills), using the formula:

$$\frac{S}{S_0} = \left(\frac{L}{L_0}\right)^{\alpha}$$

- Residual long term drifts of the individual crystal response remain after the laser corrections, which are due to different effects. (*e.g.* the values of α could be slightly different for each crystal, or other ageing effects ...)
- These effects can be monitored and corrected for using physics channels, *e.g.* by exploiting the azimuthal symmetry of the energy deposits in minimum bias events.

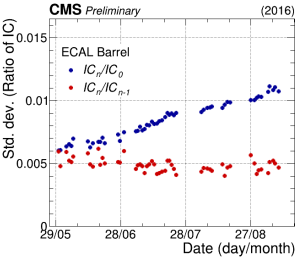

Plots on the left (barrel) and right (endcap), show the dispersion of the inter-calibration coefficients versus time during 2016 data taking, obtained with the azimuthal symmetry method.

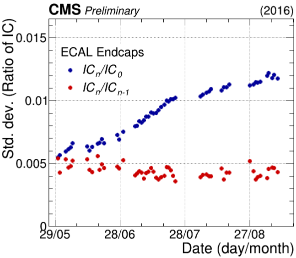

Inter-calibration: Methods

- We use three methods to inter-calibrate crystal response.
  1. $\pi^0 \rightarrow \gamma\gamma$ energy distribution peak
  2. Comparing reconstructed energy with independent measurement of momentum from tracker
  3. $Z \rightarrow ee$ distribution
- Each method gives independent inter-calibration coefficients which we then combine for a final measurement.

Inter-calibration method 1: $\pi^0 \to \gamma\gamma$

- One can use the reconstructed invariant masses of photon pairs from π^0 to inter-calibrate crystal response, using:

Method

The peak of the fitted $m_{\gamma\gamma}$ distribution is ensured to be the same value for each crystal.

- For each crystal, we obtain this fit using all events with one hit in that crystal. Then,

$$C_i = \frac{m_{\pi^0}\,(\text{measured with crystal } i)}{m_{\pi^0}\,(\text{PDG})}$$

- Repeated iteratively until convergence.
- Dataset: Special stream of data from dedicated trigger that selects diphoton events close to the π^0 resonances, allowing sufficient statistics for inter-calibration and monitoring.

Inter-calibration method 1: $\pi^0 \to \gamma\gamma$

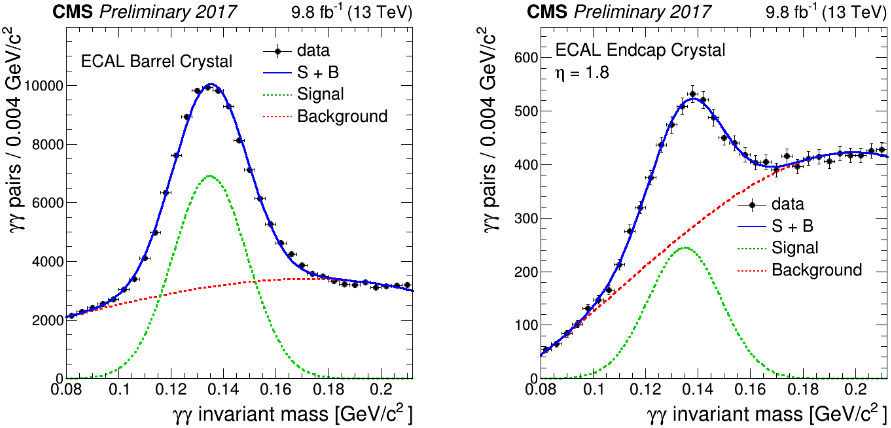

Examples of $m_{\gamma\gamma}$ distributions, with fits to the data, for selected crystals in the barrel (left) and in the endcaps (right).

Inter-calibration method 2: E/p ratio

- One can use the momentum reconstructed by the CMS tracker (strips + pixels) as a reference.

Method

The fraction E/p in each crystal is made to fit a common underlying template, where E = ECAL supercluster energy, p = tracker momentum.

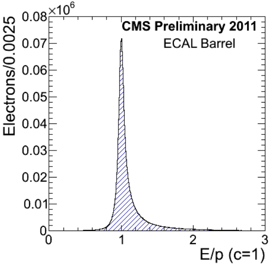

We obtain the template from a very *high purity* sample of *high energy* electrons from W/Z decay.

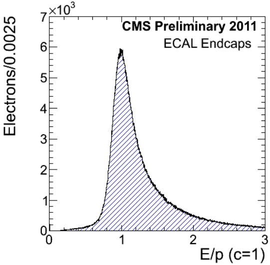

We derive the crystal inter-calibrations by iteratively scaling the coefficients C_i until the E/p distribution in each crystal converges to the template.

Inter-calibration method 3: $Z \to ee$

- One can use the known mass and lifetime of $Z \to ee$ as a reference.

Method

The overall Z-peak as reconstructed from data in all crystals is fitted to a convolution of the known natural $Z-$shape (which depends on $Z-$mass and lifetime), and a spread due to resolution effects.

- The mass and decay width of Z are obtained from PDG.
- We use a likelihood maximization algorithm, with the inter-calibration coefficients C_i as parameters.
- In addition to the inter-calibration parameters, we include the resolution in several $\eta-$ bins as parameters, allowing us to obtain estimates of the $\eta-$binned energy resolution.

Inter-calibration: Combination

Assuming no correlation between the three different methods used to inter-calibrate crystal response, we have: (n.b. both systematic and statistical uncertainty are included in the estimates of the precision)

$$\begin{aligned} \sigma_1^2 + \sigma_2^2 &= \sigma_{1-2}^2 \\ \sigma_1^2 + \sigma_3^2 &= \sigma_{1-3}^2 \\ \sigma_2^2 + \sigma_3^2 &= \sigma_{2-3}^2 \end{aligned} \quad \Longrightarrow \quad \begin{aligned} \sigma_1^2 &= \frac{1}{2}\left(\sigma_{1-2}^2 + \sigma_{1-3}^2 - \sigma_{2-3}^2\right) \\ \sigma_2^2 &= \frac{1}{2}\left(\sigma_{2-3}^2 + \sigma_{1-2}^2 - \sigma_{1-3}^2\right) \\ \sigma_3^2 &= \frac{1}{2}\left(\sigma_{1-3}^2 + \sigma_{2-3}^2 - \sigma_{1-2}^2\right) \end{aligned}$$

Finally the combined inter-calibration value for each crystal is obtained as the weighted mean of the values obtained by each individual method.

Note: For the endcaps in 2017, we only use the $Z \to ee$ method because it is much more precise than the other methods; therefore, we do not have estimates of the precision from the system of equations.

Inter-calibration: 2017 Precision

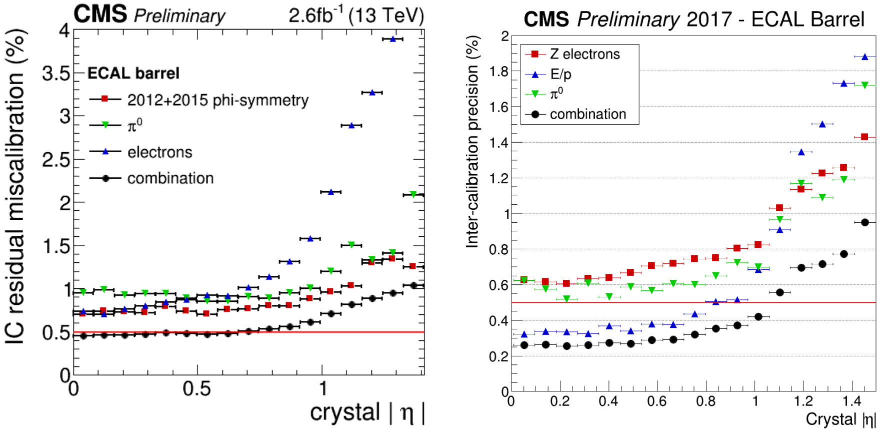

Individual and combined inter-calibration precision: compare 2015 results (on the left) with 2017 results (on the right). For 2017 results, the precision from $Z \rightarrow ee$ and $\pi^0 \rightarrow \gamma\gamma$ decays is at the level of the systematic error, while the statistical errors are still dominant for the E/p precision at $|\eta| > 1$. The black points represent the combined weighted precision.

Preshower calibration

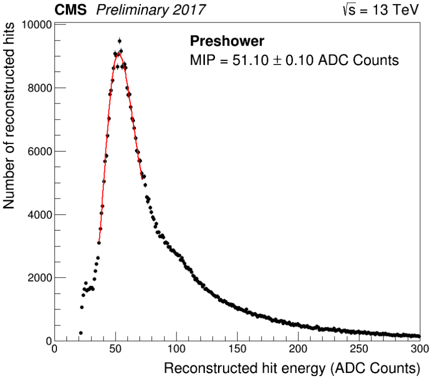

Fitted around the peak to a Landau convoluted with a Gaussian.

- Calibration of the preshower involves calculating the conversion from ADC counts to GeV.
- A few times per year we take a special run with the preshower in high gain mode; this allows us to see the MIP peak and calibrate the preshower sensors.
- We reconstruct MIP peak per channel → gives ADC-to-MIP conversion.
- MIP-to-GeV conversion is known: 1 MIP $= 80.4\,\mathrm{keV}$

Preshower MIP stability

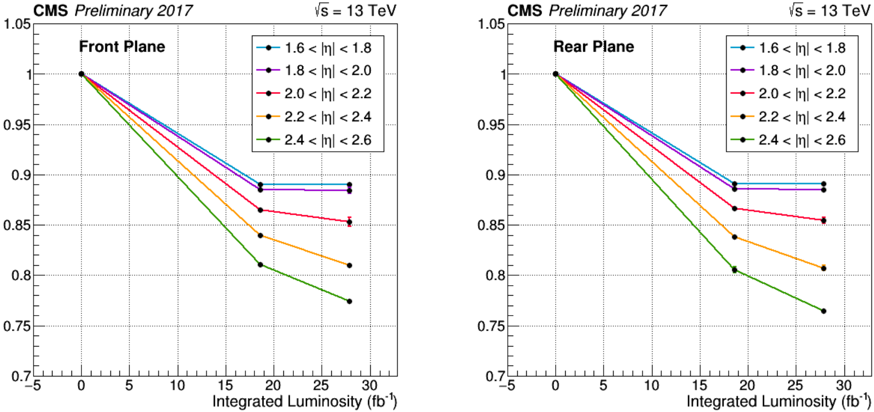

MIP response evolution with respect to beginning of 2017 in the preshower.

ES sensors in high η regions are affected more by radiation damage.

Outline

1. Introduction
   - ECAL Building Blocks
2. Calibration
   - Inter-calibration: Motivation
   - Inter-calibration: Methods
   - Inter-calibration: Results
   - Preshower Calibration
3. Monitoring and Validation using physics events
   - Motivation and methods
   - Energy scale
   - Shower shape
4. Summary

Motivation and Methods

- **Monitoring**: To ensure that reconstruction is stable throughout the year, we monitor some quantities obtained from reconstructed physics objects.
- **Validation**: At the end of the year, we apply all corrections (laser monitoring, inter-calibration coefficients, etc.), and plot the same quantities over the year, expecting that there should be no drift.
- **Quantities Monitored**:
  1. Energy scale: π^0-mass, $Z \to ee$
  2. Shower shapes: $Z \to ee$

π^0-mass

Validates: Energy Scale

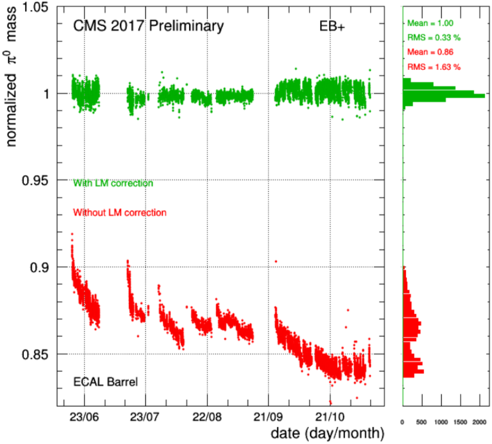

The relative energy scale measured from the invariant mass distribution of $\pi^0 \to \gamma\gamma$ decays in the ECAL Barrel remains stable throughout the year after applying transparency corrections (more on laser corrections in Amina's talk).

$Z \to ee$ invariant mass

Validates: energy scale

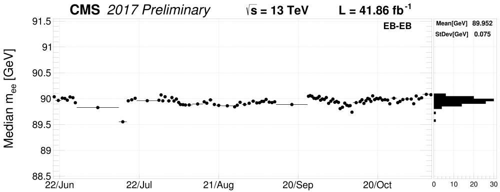

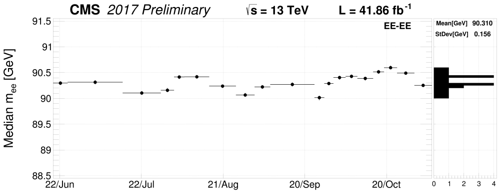

The invariant mass in $Z \to ee$ events is observed to be stable throughout the year once all corrections have been applied.

$Z \to ee\ R_9$

Validates: shower shape stability

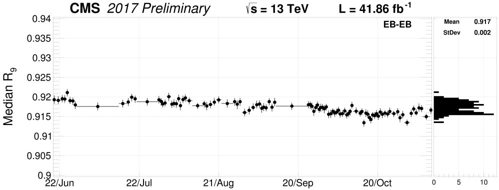

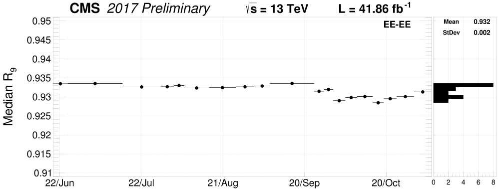

The variable $R_9 \equiv \frac{E_{3\times3}}{E_{SC}}$ is one of the variables typically used in CMS physics analyses to identify EM showers using their shower shape. It stays stable throughout the year in $Z \to ee$ events.

Outline

Performance of 2017 calibration

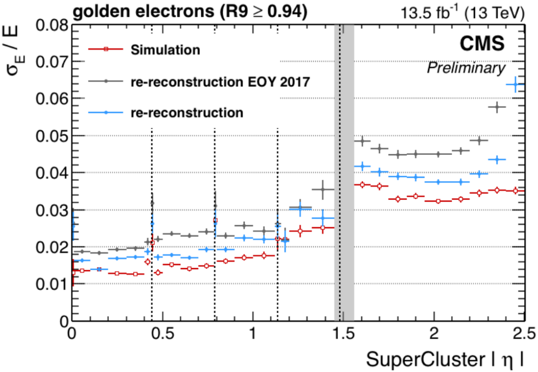

Black: reconstruction performed just at the end of data-taking; only low level parameters were optimized for this reconstruction with respect to the prompt processing due to short available time (pedestals, laser correction, timing, . . .)

Blue: reprocessing done with the new 2017 calibrations.

Reconstruction with the latest calibrations significantly improves the resolution.

Performance of 2017 calibration

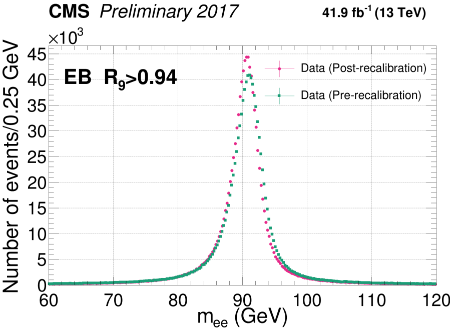

The Z-mass peak is visibly improved by updating the calibration.

Summary

- The LHC environment in 2017 has been challenging with high instantaneous luminosity, high pile-up and varying bunch filling schemes.
- The ECAL pulse amplitude reconstruction is robust with respect to pile-up effects and the many validation and monitoring methods that we have developed allow to follow and correct the evolution of the calorimeter.
- Thanks to the high integrated luminosity collected in 2017, we have calibrated the CMS ECAL exploiting many physics channels, including for the first time $Z \rightarrow ee$ at single crystal granularity.
- The new calibrations allow us to achieve a very good energy resolution in both the Barrel and the Endcaps.

BACKUP SLIDES

Inter-calibration using ϕ-symmetry

- Because of the symmetry of the CMS and ECAL around the beam axis, over a long enough time period:

Assumption

The net energy flux through a crystal should be independent of the polar angle ϕ of the crystal.

- The coefficients C_i are then set such that in each η-ring, the average of the coefficients over all crystals is 1; allows for precise inter-calibration along ϕ but not along η.

ECAL Alignment: EB + EE

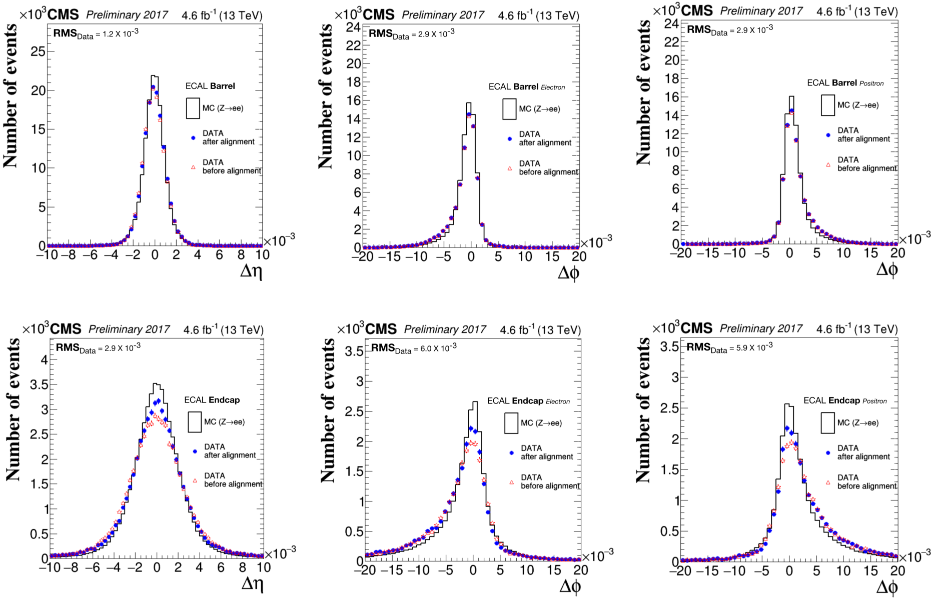

ES Alignment

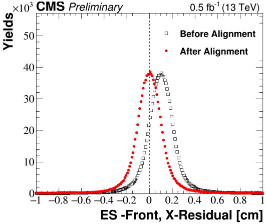

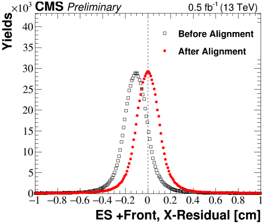

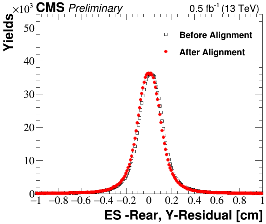

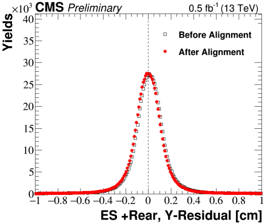

Timing

Validates: pulse shapes, rechit reconstruction

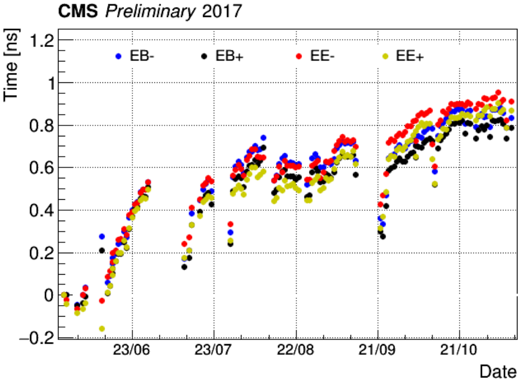

The timing drifts slightly throughout the year; however, this quantity is regularly monitored and pulse shapes are kept up-to-date to ensure that physics analyses are not affected.

Crystal noise

Validates: shower shape, lepton isolation

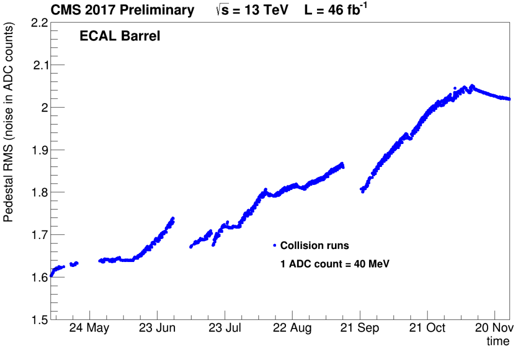

The RMS of the readout in absence of signal is a measure of the noise and slowly drifts upwards with radiation-induced damage to the APDs.

Measuring deposited energy

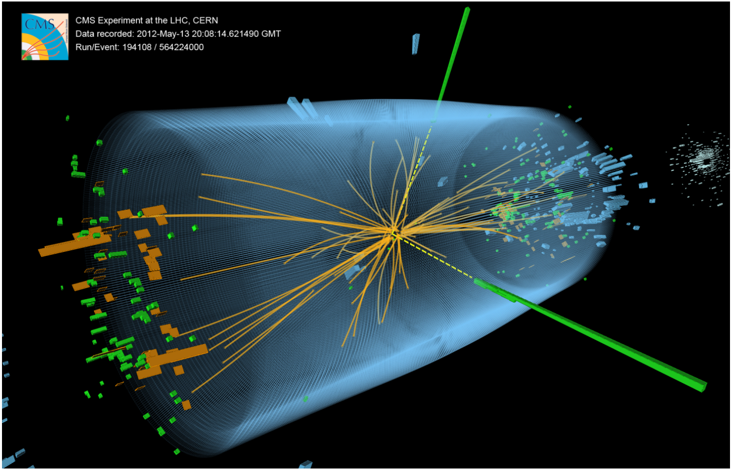

(Candidate $H \to \gamma\gamma$ event)

The energy reconstruction algorithm assigns an energy to an observed collection of crystal deposits.

Inter-calibration: more on E/p

$$C_i^{\mathrm{N}} = C_i^{\mathrm{N}-1} \times \frac{\sum\limits_{\text{good electrons}} F_i \times P\left(E_{\mathrm{SC}}^{\mathrm{N}-1} | p_{\mathrm{trk}}\right) \times \frac{p_{\mathrm{trk}}}{E_{\mathrm{SC}}^{\mathrm{N}-1}}}{\sum\limits_{\text{good electrons}} F_i \times P\left(E_{\mathrm{SC}}^{\mathrm{N}-1} | p_{\mathrm{trk}}\right)}$$

$$\begin{aligned} \text{superscript N},\ \mathrm{N}-1 &= \text{iteration index} \\ F_i &= \text{fraction of } E_{\mathrm{SC}} \text{ in crystal } i \\ P\left(E_{\mathrm{SC}} | p_{\mathrm{trk}}\right) &= \text{probability of } E_{\mathrm{SC}} \text{ given } p_{\mathrm{trk}} \\ & \quad \text{(as found from } (E/p) \text{ template)} \end{aligned}$$

Inter-calibration: more on $Z \to ee$

- Likelihood function:

$$\mathcal{L} = \prod_{Z \to ee \text{ events}} \text{Voigt}\left(m_{ee}, \sigma_{ee}, M_Z, \Gamma_Z\right)$$

where

$$\begin{aligned} m_{e_1 e_2} &= \sqrt{2 \times E_{\text{corrected}}\left(e_1\right) \times E_{\text{corrected}}\left(e_2\right) \times \left(1 - \cos\theta_{12}\right)} \\ \sigma_{e_1 e_2} &= \frac{1}{2} \times M_Z \times \left(\frac{\sigma_E}{E}\left(e_1\right) \bigoplus \frac{\sigma_E}{E}\left(e_2\right)\right) \\ E_{\text{corrected}} &= \frac{E_{ECAL}}{r\left(\eta\right)} + E_{\text{Preshower}} \end{aligned}$$

- Note that this also allows us to extract the energy resolution binned in η.